Paper 2022-17-13

New Protocol at Fast Scan Mode for Sea-surface Small Target Detection

Sangbin Cha, Sanghong Park, Jooho Jung, Inoh Choi*

Abstract : In this article, we propose a new protocol at fast scan mode for a sea-surface small target detection. The conventional fast scan mode is composed of coherent intrascan integration to suppress sea clutter and non-coherent interscan integration to exclude sea spikes. The proposed method realizes the coherent interscan integration by the new Fourier relationship between carrier-frequency and initial-radial-range, which can be analytically derived by using multiple carrier frequencies at fast scan mode, leading to improved detection performance, compared to the conventional non-coherent methods. In simulations, our proposed method is verified.

Keywords : New Fourier relationship, Carrier-frequency, Initial-radial-range, Fast scan mode, Interscan integration.

Ⅰ. Introduction

Detection of a small target (e.g., periscope, lifeboat, and iceberg) with low velocity and low radar cross section (RCS) in a maritime environment is important task for military and civil purposes [1, 2]. Detection performance depends upon signal-to-clutter ratio (SCR) of echoes received from the sea-surface small target [3]. Unfortunately, the false detection inevitably occurs due to the degradation of SCR by sea clutter and sea spikes, which leads to the difficulty of sea-surface small target detection [4].

For improved detectability, a maritime radar utilizes a fast scan mode (Fig. 1), which is composed of coherent intrascan integration to suppress sea clutter and non-coherent interscan integration to exclude sea spikes [5]. Recently, the generalized likelihood ratio test linear-threshold detector (GLRT-LTD) [5, 6] realizes optimal coherent processing in the intrascan integration based on Fourier relationship between pulse-time and radial- velocity. However, conventional interscan integration methods, such as retrospective filter bank [7] and Doppler -guided retrospective filter detector [5], are implemented by complicated non-coherent processing to exclude sea spikes, so they require computational burden.

In this article, we suggest a new protocol that uses multiple carrier frequencies to derive new Fourier relationship between carrier- frequency and initial-radial - range, leading to improved sea-surface small target detection performance, compared to conventional detection methods [5, 7]. In simulations, our proposed method is verified by using a point scatterer model for a small target and sea clutter model in [5].

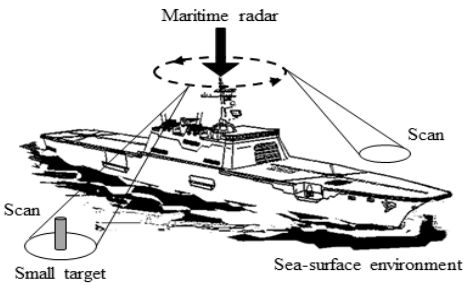

Fig. 1. Configuration of fast scan mode.

Ⅱ. Echo signal model and discussion

1. Sea clutter echo at fast scan mode

Referring to the compound-Gaussian model of sea clutter [5], sea clutter echo $c(n\Delta r,\ m\Delta t,\ l\Delta t_s)$ at fast scan mode consists of texture $\tau(n\Delta r,\ m\Delta t,\ l\Delta t_s)$, speckle $u(n\Delta r,\ m\Delta t,\ l\Delta t_s)$, and sea spikes $sp(n\Delta r,\ m\Delta t,\ l\Delta t_s)$ as

$$c(n\Delta r,\ m\Delta t,\ l\Delta t_s) = \{\tau(n\Delta r,\ m\Delta t,\ l\Delta t_s)\}^{0.5} \times u(n\Delta r,\ m\Delta t,\ l\Delta t_s) + sp(n\Delta r,\ m\Delta t,\ l\Delta t_s), \quad (1)$$

where n is the radial-range number, Δr is the

*Corresponding Author (inohchoi@kmou.ac.kr)
Received: Feb. 4, 2022, Revised: Feb. 23, 2022, Accepted: Feb. 25, 2022.
S.B. Cha: Pukyong University (Ph.D. Student)
S.H. Park: Pukyong University (Prof.)
J.H. Jung: Kookmin University (Resea. Prof.)
I.O. Choi: Korea Maritime & Ocean University (Assis. Prof.)
※ This work was supported by the National Research Foundation of Korea (NRF) grant funded by the Korea government (MSIT) (No. 2022R1G1A1004830).

ISSN : 1975-5066
http://dx.doi.org/10.14372/IEMEK.2022.17.2.101

radial-range resolution, m is the pulse number, Δt is the pulse repetition interval (PRI), l is the scan number, and Δt_s is the scan repetition interval (SRI) ($\Delta t \ll \Delta t_s$).

In (1), the texture $\tau(n\Delta r,\ m\Delta t,\ l\Delta t_s)$ can be modeled by the inverse gamma (IG) probability density function $p(\tau \mid \lambda, \eta)$ with a scale parameter η and a shape parameter λ as

$$\begin{aligned}\tau(n\Delta r,\ m\Delta t,\ l\Delta t_s) &\sim p(\tau \mid \lambda,\eta),\\ &= \frac{1}{\Gamma(\lambda)}\left(\frac{\lambda}{\eta}\right)^{\lambda}\frac{1}{\tau^{\lambda+1}}exp\left(-\frac{\lambda}{\eta\tau}\right),\end{aligned} \tag{2}$$

where $\Gamma(\lambda)=(\lambda-1)!$ is the gamma function. To express the time-evolving sea-surface (i.e., structural trend) in the texture, the RCS map computed by a computational electromagnetics tool is required with the simple combining process in [5] (refer to [5] in detail).

Next, the speckle $u(n\Delta r,\ m\Delta t,\ l\Delta t_s)$ is independent on $n\Delta r$ and $l\Delta t_s$ (i.e., $u(n\Delta r,\ m\Delta t,\ l\Delta t_s) = u(m\Delta t)$), which can be modeled as follows:

$$u(m\Delta t) = u_0(m\Delta t)\times \exp\left(j2\pi m\Delta t f_d(m\Delta t)\right), \tag{3}$$

where $u0(m\Delta t)$ is the output of the first order auto regressive (AR) process with a zero-mean unit-variance white Gaussian input $w(m\Delta t)$ and a one-lag correlation coefficient ρ as

$$u_0((m+1)\Delta t) = \rho\, u_0(m\Delta t) + \sqrt{1-\rho^2}\, w(m\Delta t), \tag{4}$$

and $f_d(m\Delta t)$ is the Doppler frequency shift of speckle correlated with relative intensity of texture (refer to [5] in detail).

Finally, the sea spike $sp(n\Delta r,\ m\Delta t,\ l\Delta t_s)$ is independent on $l\Delta\theta$ (i.e., $sp(n\Delta r,\ m\Delta t,\ l\Delta t_s) = sp(n\Delta r,\ m\Delta t)$), which can be represented by

$$\begin{aligned}sp(n\Delta r,\ m\Delta t) &= A_{sp}\times\exp\left(\frac{j4\pi f_c v_{sp}(m-m_0)\Delta t}{c}\right)\\ &\times\Psi\left(\frac{(n-n_0)\Delta r - v_{sp}(m-m_0)\Delta t}{L_{sp}}, \frac{(m-m_0)\Delta t}{T_{sp}}\right),\end{aligned} \tag{5}$$

where f_c is the carrier frequency of radar, c is the velocity of light, A_{sp}, v_{sp}, L_{sp}, T_{sp}, and (n_0, m_0) are the amplitude, the radial-velocity, the range-length, and the life-time, and the occurrence position of sea spike, respectively (refer to [5] in detail).

2. Small target echo at fast scan mode

Assuming that the small target on a sea-surface exists in a single radial-range cell as a point scatterer, its echo is represented by

$$\begin{aligned}s(n\Delta r,\ m\Delta t,\ l\Delta t_s) &= \sqrt{E\{\tau\}\times 10^{SCR/10}}\times a(m\Delta t)\\ &\times\delta(n\Delta r - r(m,l))\exp\left(\frac{j4\pi f_c r(m,l)}{c}\right),\end{aligned} \tag{6}$$

where $E\{\tau\}=\lambda/\{\eta(\lambda-1)\}$, $1<\lambda<\infty$, is the ensemble average power of the texture [5], SCR is the SCR in decibels, $a(m\Delta t)$ is the amplitude fluctuation generated by the AR process in [5] (refer to [5] in detail), $\delta(\ )$ is the direc-delta function, and the radial-range trajectory $r(m,l)$ is simply modeled by using the initial-radial-range R_0 and the constant radial-velocity v_0 as follows:

$$r(m,l) = R_0 + v_0 m\Delta t + v_0 l\Delta t_s. \tag{7}$$

3. Discussion on sea-surface small target detection at fast scan mode

For maritime radar at fast scan mode, sea-surface small target detection is conducted by two steps: intrascan integration to suppress sea clutter and find small target candidates using GLRT-LTD in [6] (refer to [6] in detail) based on Fourier relationship between pulse-time and radial-velocity; interscan integration to exclude sea plikes and determine the final small target using the non-coherent processing algorithms in [5, 7] (refer to [5, 7] in detail). However, the conventional interscan integration methods require high computational cost due to complicated non-coherent processing algorithm. In addition, non-coherent integration definitely causes relative SCR loss, compared to coherent integration. Therefore, to improve the computation cost and SCR, we devised a new coherent interscan integration.

Ⅲ. Proposed method

1. Representation of new Fourier relationship

Assuming that small target echo is obtained using L stepped carrier frequencies $f_c(0)+(l-1)\Delta f_c$ with an initial carrier frequency $f_c(0)$ and a sampling interval Δf_c at each scan l = 1, 2, ..., L, the echo in (6) can be reformulated by

$$\begin{aligned}s(n\Delta r,\ m\Delta t,\ l\Delta f_c) &= A(m\Delta t)\times\delta(n\Delta r - r(m,l))\\ &\times rect\left(\frac{m\Delta t}{T_{CPI}}\right)\exp\left(\frac{j4\pi l\Delta f_c v_0 m\Delta t}{c}\right)\\ &\times rect\left(\frac{l\Delta f_c}{BW_c}\right)\exp\left(\frac{j4\pi l\Delta f_c R_0}{c}\right),\end{aligned} \tag{8}$$

where $A(m\Delta t)=\sqrt{E\{\tau\}\times 10^{SCR/10}}\times a(m\Delta t)$, T_{CPI} is the coherent processing interval (CPI), $rect(t)$ is the rectangular function that is 1 for $-0.5\le t\le 0.5$ for and 0 elsewhere, and $BW_c=(L-1)\Delta f_c$ is the bandwidth of carrier frequency.

After appying Fourier transform (i.e., $m\Delta t \rightarrow V$) along pulse-time $m\Delta t$ direction to (8), the echo can be expressed as

$$\begin{aligned} s(n\Delta r,\ V,\ l\Delta f_c) &= A(m\Delta t)\times\delta(n\Delta r-r(m,l)) \\ &\times\sqrt{M}\times sinc\left(\frac{2l\Delta f_c T_{CPI}}{c}m\right)\times\delta(V-v_0) \\ &\times rect\left(\frac{l\Delta f_c}{BW_c}\right)\exp\left(\frac{j4\pi l\Delta f_c R_0}{c}\right), \end{aligned} \tag{9}$$

where $V\,(=m\Delta v)$ is the radial-velocity axis with the radial-velocity resolution Δv, M is the number of pulses during a CPI, and $sinc(x)=\sin(\pi x)/\pi x$ is the sinc function. This Fourier relationship between pulse-time $m\Delta t$ and radial-velocity V is utilized to implement the conventional coherent intrascan integration (i.e., GLRT-LTD [6]) at fast scan mode, so the maximum instantaneous power of the small target echo is increased by the coherent intrascan integration from $\{A(m\Delta t)\}^2$ to $\{A(m\Delta t)\}^2\times M$.

Note that the use of multiple carrier frequencies at each scan leads to the new Fourier relationship between carrier-frequency $l\Delta f_c$ and initial-radial-range $R\,(=l\Delta R)$ can be defined as

$$l\Delta f_c \Leftrightarrow \frac{2}{c}R, \tag{10}$$

so the echo in (9) is analytically represented applying Fourier transform (i.e., $l\Delta f_c \rightarrow R$) along carrier-frequency direction $l\Delta f_c$ as follows:

$$\begin{aligned} s(n\Delta r,\ V,\ R) &= A(m\Delta t)\times\delta(n\Delta r-r(m,l)) \\ &\times\sqrt{M}\times sinc\left(\frac{2l\Delta f_c T_{CPI}}{c}m\right)\times\delta(V-v_0) \\ &\times\sqrt{L}\times sinc\left(\frac{2BW_c}{c}l\right)\times\delta(R-R_0), \end{aligned} \tag{11}$$

so the maximum instantaneous power of the small target echo is increased as much as $10\log_{10}L$ in decibels, unlike the conventional non-coherent interscan integration in [5, 7]. In addition, the SCR may be more increased because the sea clutter echo in (1) is more uncorrelated by different carrier frequencies at each scan.

2. Detection protocol at fast scan mode

In our work, the intrascan integration step at fast scan mode is achieved by using the conventional optimal coherent detector (i.e., GLRT-LTD) [6]. For that, we define the Doppler steering vector $\vec{p}$ as

$$\vec{p} = [1, e^{j2\pi f_d(m)\Delta t},\ldots,e^{j2\pi f_d(m)\Delta t(M-1)}]^T, \tag{12}$$

where $f_d(m)=(m-1)/T_{CPI}$, $m=1, 2, \ldots, M$, and ^{T} is the transpose operator. When the $M\times 1$ received echo vector $\vec{y}$ is obtained from (8) at the instantaneous radial-range and scan-time, N_c candidates can be detected by using the conventional GLRT-LTD [6] with the hypothesis test (i.e., H_1 : small target with sea clutter and H_0 : only sea clutter) as

$$\frac{\left|\vec{p}^H\mathbb{M}^{-1}\vec{y}\right|^2}{\left(\vec{p}^H\mathbb{M}^{-1}\vec{p}\right)\left(\lambda/\eta+\vec{y}^H\mathbb{M}^{-1}\vec{y}\right)} \underset{H_0}{\overset{H_1}{<>}} 1-P_{fa}^{\left(\frac{1}{M+\lambda-1}\right)}, \tag{13}$$

where $\mathbb{M}$ is the estimated $M\times M$ covariance matrix of the speckle at the reference cells [6], P_{fa} is the false alarm probability, and ^{H} is the Hermitian operator.

For the new coherent interscan integration at fast scan mode, we adopt the simple maximum peak selection approach in a initial-radial-range domain defined by the new Fourier relationship. This process is implemented by using (11) at the instantaneous radial-range and radial-velocity of the N_c candidates detected by the coherent interscan integration step.

Ⅳ. Simulation results

In this section, we utilized a recent simulation method in [5] to generate the sea clutter data because open databases are quite a few, so it is difficult to collect those.

1. SCR improvement

To verify the effectiveness of the proposed method, we utilized the compound-Gaussian model and a point scatterer model for sea clutter and small target with the parameters (Table 1 and 2) corresponding to a realistic situation, respectively. The maritime radar is assumed to be located at an altitude of 20 m and has a beamwidth of 1.44°, 250 beam positions along azimuth direction from 0° to 360°. This radar transmits 8 coherent pulses (i.e., dwell time = 4 msec and frame time = 250 × 4 msec = 1 sec) at each beam position, 30 scans at 60 rotations per minute

Table 1. Simulation parameters for sea clutter and small target.

Scale parameter η	1
Shape parameter λ	1.5
Average power $E\{\tau\}$	3 W
Velocity of sea spike v_{sp}	0.15 m/s
Range-length of sea spike L_{sp}	5 m
Life-time of sea spike T_{sp}	0.15 sec
SCR	10 dB
Initial-radial-range R_0	8.5 km
Constant radial-velocity v_0	5 m/s

Table 2. Simulation parameters for radar.

Initial carrier frequency $f_c(0)$	3 GHz
Carrier frequency interval $\triangle f_c$	10 kHz
Radial-range resolution $\triangle r$	300 m
PRI $\triangle t$	0.5 msec
CPI T_{CPI}	4 msec
SRI $\triangle t_s$	1 sec
M	8
L	30

(rpm), and searches for the sea-surface covering the radial-range from 0 to 15 km.

The echoes returned from the small target (Fig. 2) were obtained for the point scatterer model. Here, the instantaneous power of single pulse returned from the target was 14.77 dBW, however, after appying coherent intrascan integration (e.g., Fast Fourier transform (FFT)) along pulse-time m$\triangle t$ direction, the instantaneous power was increased as much as $20\log_{10}M = 20\log_{10}8 = 18.06$ in decibels due to coherent processing gain by 8 pulses. In addition, the proposed scheme that uses multiple carrier-frequencies contributes to the additional coherent processing gain by 30 scans (i.e., $20\log_{10}L = 20\log_{10}30 = 30.54$ dBW), unlike convention methods [5, 7].

The echoes returned from the sea-surface (Fig. 3) were obtained by using the sea clutter model in [5]. Generally, the ensemble averaging power of the sea clutter model in [5] can be defined as $E\{\tau\} = \lambda/\{\eta(\lambda-1)\}$ of the texture τ in (2). In our work, the sample averaging power of the echoes was utilized, so the averaging power of the sea clutter in a radial-range and pulse-time domain was 4.77 dBW, resulting in SCR = 10 dB when the instantaneous power of the target's echo is 14.77 dBW. Next, after appying coherent intrascan integration along pulse-time m$\triangle t$ direction, the averaging power of the sea clutter in a radial-range and radial-velocity domain was increased as much as 6.94 dBW because each pulse returned from the sea-surface is correlated in a time

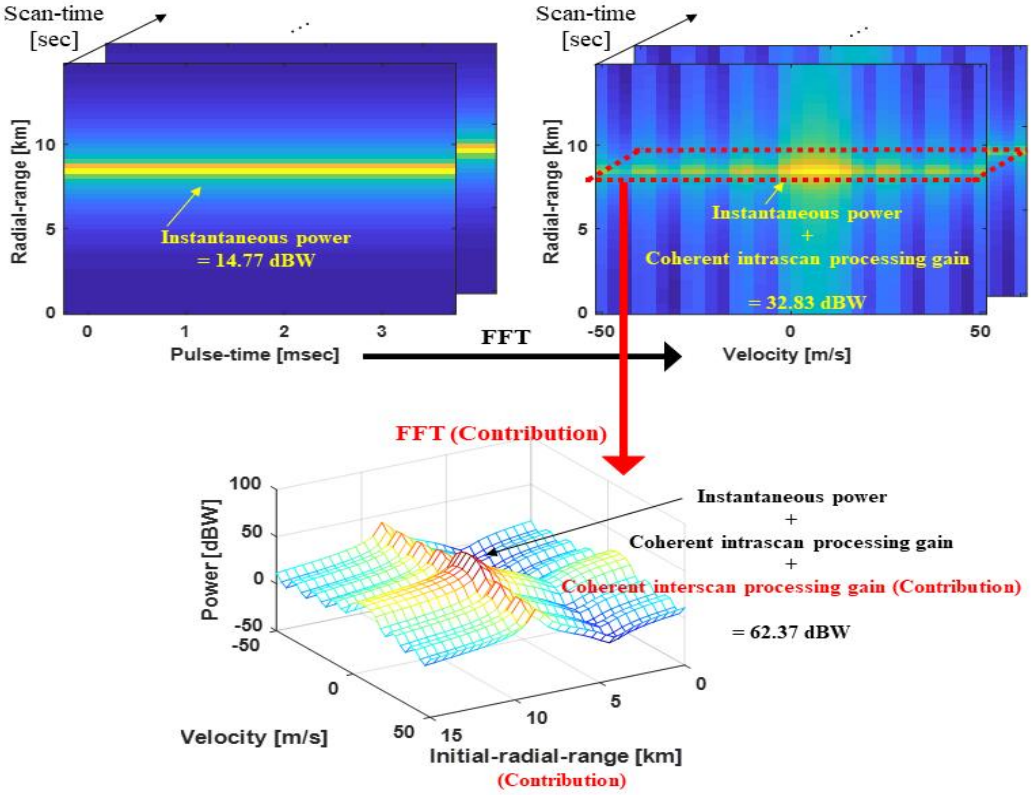

Fig. 2. Example of echoes returned from the small target.

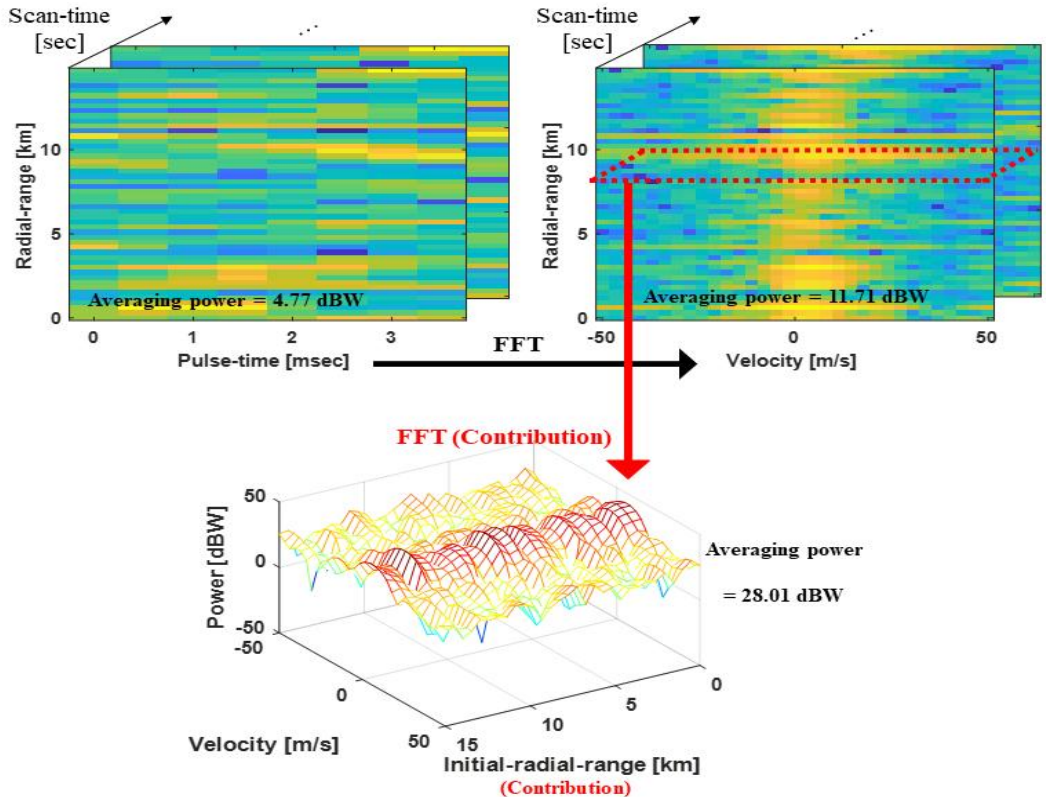

Fig. 3. Example of echoes returned from the sea-surface.

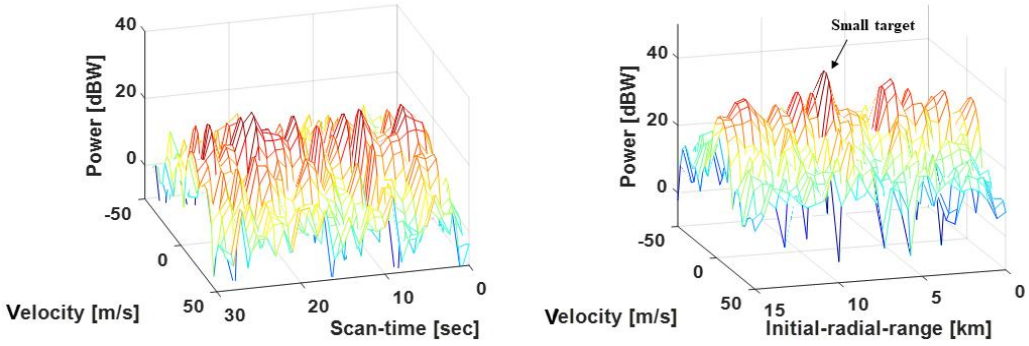

(a) (b)

Fig. 4. Example of echoes returned from a sea-surface small target at SCR = - 5 dB.
(a) Echoes in a radial-velocity and scan-time. (b) Echoes in a radial-velocity and initial-radial-range.

interval of the order of seconds, so the Doppler power spectrum of the sea clutter is defined as a unimodal bell-shaped function [5]. In this case, the SCR was increased as much as 21.12 dB due to the coherent processing gain of the target's echo, but sometimes a few strong outliers (e.g., structural trend and sea spike) occur, leading to false detection problem.

Here, the proposed scheme realizes the additional coherent processing along carrier-frequency $1\triangle f_c$ direction, so the SCR becomes 34.36 dB: the instantaneous power of target = 62.37 dBW; the averaging power of sea cluter = 28.01 dBW.

Fig. 4 (a) presents the echoes in a radial-velocity and scan-time at SCR = - 5dB, which is used to detect the small target by the conventional methods in [5, 7]. Unfortunately, the conventional methods can no longer detect the small target due to strong sea clutter. In contrast, Fig. 4 (b) shows the echoes in a radial-velocity and initial-radial-range at SCR = - 5dB, which can be more effectively used for the sea-surface small target

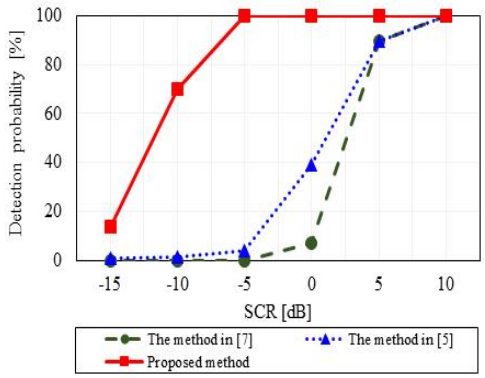

Fig. 5. Quantitative evaluation of detection performance for conventional methods in [5, 7] and the proposed method.

detection by the improved SCR. Therefore, the small target in a sea clutter environment can be robustly detected by using the proposed protocol.

2. Detection performance

For a quantitative comparison of the detection performance of the proposed method and the conventional methods in [5, 7], we considered the several simulation data samples for SCRs from -15 to 10 dB in increments of 5 dB; for each SCR. we conducted 50 Monte Carlo simulations by adding the independent sea clutter. As a useful measure to describe the quality of the detection performance, we computed the detection probability for 50 Monte Carlo simulations. The proposed method had much high detection probability than the conventional methods in [5, 7] at all SCRs (see Fig. 5) due to improved SCR by the proposed coherent processing.

For a complexity comparison, we considered the number of multiplications: conventional method is $O(M^2)$ and $O(N^2 \times L^2)$ for intrascan integration (e.g., GLRT-LTD) and interscan integration (e.g., image processing); proposed method is $O(M \times \log M)$ and $O(L^2)$ for intrascan integration (e.g., FFT) and interscan integration (e.g., GLRT-LTD). Note that the conventional methods must require high resolution radar echoes for complicated image processing, so the computational burden of the conventional methods will be larger than that of the proposed method with relatively low resolution. Furthermore, in our simulation, we used MATLAB R2019a on a computer running Window 10 with an Intel i7 processor. The computational time of the proposed method was ~ 0.09 s, whereas that of the conventional methods was ~ 0.18 s and ~ 0.23 s, respectively. Therefore, we conclude that the sea-surface small target can be detected by using the proposed protocol, with good accuracy and efficiency.

V. Conclusion

This article has presented a new protocol to detect the sea-surface small target at fast scan mode. In simulations using a point scatterer model and sea clutter model in [5], the proposed method was more accurate, robust, and efficient at detecting the small target, compared to conventional methods.

References

[1] J. M. Smith, R. H. Logan, "AN/APS-116 Periscope-detecting Radar," IEEE Transactions on Aerospace and Electronic Systems, Vol. 16, No. 1, pp. 66-73, 1980.

[2] J. Ryan, "Detection of Small Radar Cross Section Targets at sea Using Coherent Radar," International Conference on Radar Systems, pp. 23-26, 2017.

[3] Y. G. Zemskov, Y. M. Zotov, V. V. Sidorov, "Radar Locating of Small-sized Targets on the Rough sea Surface Background," Proceedings International Radar Conference, pp. 8-11, 1995.

[4] K. Gerlach, S. D. Blunt, "Radar Pulse Compression Repair," IEEE Transactions on Aerospace and Electronic Systems, Vol. 43, No. 3, pp. 1188-1195, 2007.

[5] S. N. Shi, X. Liang, P. L. Shui, J. K. Zhang, S. Zhang, "Low-velocity Small Target Detection with Doppler-guided Retrospective Filter in High Resolution Radar at Fast Scan Mode," IEEE Transactions on Geoscience and Remote Sensing, Vol. 57, No. 11, pp. 8937-8953, 2019.

[6] K. J. Sangston, F. Gini, M. S. Greco, "Coherent Radar Target Detection in Heavy-tailed Compound-Gaussian Clutter," IEEE Transactions on Aerospace and Electronic Systems, Vol. 48, No. 1, pp. 64-77, 2012.

[7] J. J. Ousborne, D. Griffith, R. W. Yuan, "A Periscope Detection Radar," Johns Hopkins APL Tehnical Dig., Vol. 18, No. 1, pp. 125-133, 1997.

Sangbin Cha (차 상 빈)

2017 Electronic Engineering from Pukyong National University, Busan, Republic of Korea (B.S.)

2019 Electronic Engineering from Pukyong National University, Busan, Republic of Korea (M.S.)

2020~Electronic Engineering in Pukyong National University, Busan, Republic of Korea (Ph.D. Student)

Career:

2019~Researcher (EM Technology Research Center in Kookmin University)

Field of Interests: Radar resource management, Radar target imaging and recognition, Radar signal processing, Target motion compensation, Pattern recognition using artificial intelligence, RCS prediction, and electromagnetic analysis of the windfarm

Email: teddy@pukyong.ac.kr

Sanghong Park (박 상 홍)

2004 Electronic Engineering from Pohang University of Science and Technology (POSTECH), Pohang, Republic of Korea (B.S.)

2007 Electronic Engineering from POSTECH, Pohang, Republic of Korea (M.S.)

2010 Electronic Engineering from POSTECH, Pohang, Republic of Korea (Ph.D.)

2010~Electronic Engineering in Pukyong National University (Prof.)

Career:

2003~2005 Hardware Engineer (Samsung Electronics Mobile Division)

2010 Brain Korea 21 Postdoctoral Fellow (Electromagnetic Technology Laboratory, POSTECH)

Field of Interests: Radar resource management, Radar target imaging and recognition, Radar signal processing, Target motion compensation, and Radar cross section prediction

Email: radar@pknu.ac.kr

Jooho Jung (정 주 호)

1995 Electronic Engineering from Seoul National University, Seoul, Republic of Korea (B.S.)

1998 Electronic Engineering from Pohang University of Science and Technology (POSTECH), Pohang, Republic of Korea (M.S.)

2007 Electronic Engineering from POSTECH, Pohang, Republic of Korea (Ph.D.)

2020~EM Technology Research Center in Kookmin University, Seoul, Republic of Korea (Resea. Prof.)

Career:

2008~2012 Lieutenant colonel (Defense Acquisition Program Administration)

2012 Resea. Prof. (Electronics Engineering in POSTECH)

2015 Resea. Prof. (Unmanned Technology Research Center in Korea Advanced Institute of Science and Technology)

Field of Interests: Radar target recognition, Radar signal processing, and Electromagnetic analysis in wind farms by various military radars

Email: Jungjooho68@gmail.com

Inoh Choi (최 인 오)

2012 Electronic Engineering from Pukyong National University, Busan, Republic of Korea (B.S.)

2014 Electronic Engineering from Pukyong National University, Busan, Republic of Korea (M.S.)

2020 Electronic Engineering from Pohang University of Science and Technology, Pohang, Republic of Korea (Ph.D.)

2021~Electronics and Communications Engineering in National Korea Maritime & Ocean University (Assis. Prof.)

Career:

2019~2021 Senior Researcher (Agency for Defense Development)

Field of Interests: Radar resource management, Micro-Doppler analysis, Ballistic target discrimination, Vital sign detection, Automotive target recognition, and Calibration of polarimetric SAR

Email: inohchoi@kmou.ac.kr